A New Protection Scheme for Three-Terminal Mutually Coupled Transmission Line

Snehal V. Unde, Pratik D. Dhopte*, Prashant N. Gawande, Sanjay S. Dambhare
Electrical Engineering Department, College of Engineering, Pune
*pratikdhopte@gmail.com

Abstract— **The paper presents a new protection scheme for three-terminal mutually coupled double circuit transmission line using time synchronized voltage and current phasors measurements. The communication-assisted distance protection schemes are extensively used for protection of these lines. The presence of a third source-terminal causes under-reach and overreaching problems and increases the challenges during the protection of these lines. The proposed protection method uses synchronized measurements of voltage and current phasors, measured at three ends of a three-terminal transmission line. These measurements are further used to calculate voltage at the tap point. Then the superimposed voltage components are calculated at the tap point and at three terminals for both the parallel circuits. The method compares a maximum among the superimposed voltage phasor component calculated at the tap point with the maximum among the superimposed voltage phasor components measured at the three terminals of the line to identify the faulty line. A 400-kV three-terminal mutually coupled double-circuit test system is simulated in ATP/EMTP environment and the scheme is verified in MATLAB. The simulation results confirm the superiority of proposed scheme.**

Keywords— Line Fault, Fault Detection, Power Swing, Three Terminal Line.

I. INTRODUCTION

To provide reinforcement through a transformer to underlying lower voltage network or to connect loads intermediately, transmission lines are occasionally tapped. This is called multi-terminal transmission lines. Multi-terminal lines are often designed for strengthening the power system as a provisional, low-cost measure. To exploit the technical, economic and environmental benefits over two terminal lines, three-terminal lines are used. Hence it is used at sub-transmission and transmission levels. A three-terminal line is the most used topology among different multi-terminal configurations. Due to environmental and economic constraints, there is limited availability of transfer corridors. Hence, there is an increasing trend for using multi-circuit transmission lines.

The existing protection schemes have some challenges when used for protecting a three-terminal mutually coupled transmission line [1]. During outfeed condition, protection of three-terminal lines using distance relay has an overreaching problem. The presence of third source-terminal causes under reach for line faults beyond the tap point. Current differential protection while protecting long transmission line has problems because of high charging current, current transformer saturation and unequal line impedances [2]. Unit protection scheme or communication assisted distance protection schemes [3] such as, Direct Under-reaching Transfer Trip (DUTT), Directional Comparison Blocking (DCB) and Permissive Overreaching Transfer Trip (POTT) [4], delivers 100% protection to three terminal lines. But, unwanted protection operation during stable power swing is the limitation of communication assisted distance protection schemes.

Power system protective relays are designed to sense the faults correctly to isolate the faulted section as early as possible. As the parameters and states of a power system vary continuously, it is difficult to incorporate all variations in relay setting that may appear. The fixed relay setting is a concern in relay performance during stressed operating conditions of a power system. The development in GPS and a communication system can provide real time synchronized phasor data of voltages and currents for monitoring power system dynamic states. With the recent advancement in computer networking, this time synchronized data can also be used for development of improved protection schemes for the protection of transmission systems.

In this paper, synchronized voltage and current phasors from all the ends of three terminal line are used. GPS is considered for time synchronization and fiber optics is considered for data communication. Mutual coupling of double circuit line is accounted for tap point voltage calculation. A superimposed component is calculated for all phases and at tap point which are used to determine faulty phases. The method compares a maximum among the superimposed voltage phasor component calculated at the tap point with the maximum among the superimposed voltage phasor components measured at the three terminals of the line. The performance of the scheme is observed for various symmetrical and unsymmetrical fault conditions. The proposed protection scheme works accurately even in the presence of the stable power swing.

II. PROPOSED SCHEME

A superimposed component of the voltage based technique in sequence domain is proposed for symmetrical fault discrimination in [5]. In this paper we further extend its application for detection of unsymmetrical faults in three-terminal mutually coupled double circuit transmission line in phase domain. A three-terminal mutually coupled double-circuit line as shown in Fig. 1 is considered to demonstrate the proposed scheme. Parameters of the system [5] are mentioned in the Appendix. *M*, *N* and *P* are the three terminals of system and *T* and *T'* represents a tap point.

978-1-5386-6159-8/18/$31.00 ©2018 IEEE

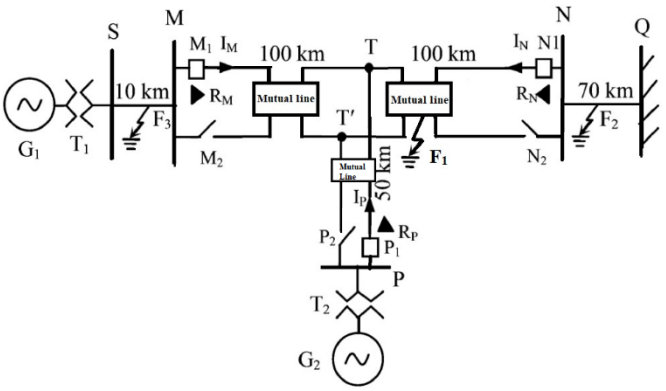

Fig. 1. Three-terminal mutually coupled double-circuit 400-kV test system [5].

Let $\bar{V}_M^{abc}$, $\bar{V}_N^{abc}$ and $\bar{V}_P^{abc}$ be the three phase synchronized voltage phasors at bus *M*, *N* and *P*. $\bar{I}_M^{abc}$, $\bar{I}_N^{abc}$ and $\bar{I}_P^{abc}$ are the three phase currents flowing through one circuit at bus *M*, *N* and *P*. Similarly, $\bar{I}_M^{abc}$', $\bar{I}_N^{abc}$' and $\bar{I}_P^{abc}$' be the corresponding currents in the other circuit. Knowing the transmission line parameters and synchronized measurements of bus voltages and currents, we can estimate the *T* point voltages seen from all the three terminals as described below.

Let $\bar{V}_{TM}^{abc}$, $\bar{V}_{TN}^{abc}$ and $\bar{V}_{TP}^{abc}$ are the estimated three phase voltage phasors at the *T* point from terminals *M*, *N* and *P*.

The *T* point voltage from any one of the end is determined using voltage drops ΔV_X^{abc}, where *X* stands for bus variable i.e. *X*= *M*, *N*, *P* [6]:

$$[\Delta V_X^{abc}] = [Z_{abc}]\,[I_X^{abc}]\,l$$

The $[Z_{abc}]$ is phase impedance matrix, $[I_X^{abc}]$ is three phase current phasors vector for the mutually coupled line and *l* is the length of the mutually coupled line segments. In the matrix form, we can elaborate the same as,

$$\begin{bmatrix}\Delta V_a\\ \Delta V_b\\ \Delta V_c\\ \Delta V_{a'}\\ \Delta V_{b'}\\ \Delta V_{c'}\end{bmatrix} = \begin{bmatrix} Z_s & Z_m & Z_m & Z_p & Z_p & Z_p\\ Z_m & Z_s & Z_m & Z_p & Z_p & Z_p\\ Z_m & Z_m & Z_s & Z_p & Z_p & Z_p\\ Z_p & Z_p & Z_p & Z_s & Z_m & Z_m\\ Z_p & Z_p & Z_p & Z_m & Z_s & Z_m\\ Z_p & Z_p & Z_p & Z_m & Z_m & Z_s\end{bmatrix}\begin{bmatrix} I_a\\ I_b\\ I_c\\ I_{a'}\\ I_{b'}\\ I_{c'}\end{bmatrix} l$$

Using the above computed voltage drops $[\Delta V_X^{abc}]$, the T point voltages seen from three terminals are estimated as below,

$$[V_{TX}^{abc}] = [V_X^{abc}] - [\Delta V_X^{abc}] \quad (1)$$

Where $[V_{TX}^{abc}]$ is *T* point voltage matrix seen from terminal X.

In absence of internal fault, tap point voltages computed from all the three ends are equal *i.e.,*

$$\bar{V}_{TM}^{abc} = \bar{V}_{TN}^{abc} = \bar{V}_{TP}^{abc}.$$

However, the computed voltages are unequal in presence of internal fault. The voltages $\bar{V}_{TM}^{abc} \neq \bar{V}_{TN}^{abc} \neq \bar{V}_{TP}^{abc}$, which will depend on fault location and type.

We then compute the three phase superimposed voltage phasors components at (*T*) point as shown below,

$$\bar{V}_{TX\,\mathrm{sup}}^{abc}(n) = \bar{V}_{TX}^{abc}(n) - \bar{V}_{TX}^{abc}(n - S) \quad (2)$$

Where S is samples per cycle and n is the time index.

The maximum among the three values of three phase superimposed voltage phasors components at the (*T*) point is the considered as,

$$g_1^{abc}(n) = max\,(|\bar{V}_{TX\,\mathrm{sup}}^{abc}(n)|) \quad (3)$$

The three phase superimposed voltage phasors components measured at the three-terminals *M*, *N* and *P* are calculated as,

$$\bar{V}_{X\,\mathrm{sup}}^{abc}(n) = \bar{V}_X^{abc}(n) - \bar{V}_X^{abc}(n - S) \quad (4)$$

The maximum among the three values of three phase superimposed voltage phasors components at bus *M*, *N* and *P* is calculated as,

$$g_2^{abc}(n) = max\,(|\bar{V}_{X\,\mathrm{sup}}^{abc}(n)|) \quad (5)$$

A difference of maximum value of superimposed voltage components are then used for an internal fault identification i. e. in case of an internal fault,

$$g_1^{abc}(n) - g_2^{abc}(n) > \xi \quad (6)$$

Where ξ is a threshold and can be decided from rigorous simulations and depends on system parameters as well as the system disturbances like stable and unstable power swing.

III. Relaying Algorithm

1. Input line parameters, sampling frequency, ξ etc.
2. Acquire the latest time tagged samples of three phase current and voltage from the buses *M*, *N* and *P*.
3. Obtain phasors using the full cycle recursive DFT for three phase current and voltage corresponding to bus *M*, *N* and *P* node.
4. Compute $V_{TM}^{abc}(t)$, $V_{TN}^{abc}(t)$, $V_{TP}^{abc}(t)$ using eq. (1) *i.e.* the T point votage where *a, b* and *c* specifies the three phases.
5. Compute the superimposed voltage phasors components measured at bus *M*, *N* and *P.* Then calculate the maximum among all of them i.e. $g_2(n)$ corresponding to *a, b* and *c* three phases.
6. Compute the superimposed voltage phasors components calculated at *T* point and maximum of them i.e. $g_1(n)$ corresponding to *a, b* and *c* three phases.
7. If, $g_1^{abc}(n) - g_2^{abc}(n) > \xi$, then trip on internal fault, else, no trip.

IV. Simulation Results

A 400 kV, three-terminal mutually coupled double-circuit transmission line is modeled and simulated in EMTP/ATP. Using data generated from EMTP/ATP proposed scheme is implemented in MATLAB.

The availability of Fiber Optic Link (FOL) is considered between terminals *M*, *N* and *P*. Full cycle recursive DFT is used to compute voltage and current phasors. Using the corresponding a, b and c three phases voltage phasors and three phase current phasors, *T* point three phase voltage phasor is calculated. The value of ξ varies with system configurations and is found to be 8 kV for this system. The internal faults are then identified using the proposed algorithm and appropriate line trip decisions are executed.

Performance of scheme is evaluated for different internal and external faults like LLG, LLL, SLG, LL as well as other disturbances.

978-1-5386-6159-8/18/$31.00 ©2018 IEEE

Further, the stable power swing is created by operating breakers at M_1, N_1 and P_1 and performance of proposed algorithm is evaluated for internal and external faults.

A. External Faults:

The proposed algorithm is tested for various external faults. The fault location and fault resistance are also varied. We present the results of various external faults like SLG, LL, LLG, LLL etc. with 10 Ω per phase resistance, created at 20 km distance from node N toward bus-Q at F_2.

1) Case-1: During External SLG fault: SLG fault is created on phase a at 4.2 s at F_2. Because it is external fault, the value of $(\mathcal{g}_1^a - \mathcal{g}_2^a)$ for phase a does not exceed ξ. Figure 2 shows that for such a fault, $(\mathcal{g}_1^a - \mathcal{g}_2^a)$ of phase a is well below ξ.

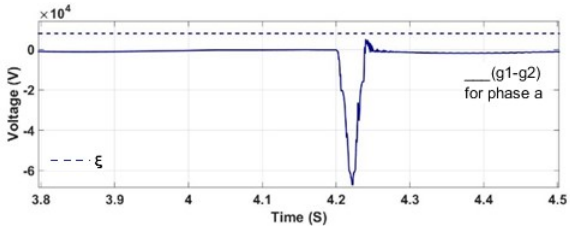

Fig. 2. Performance of proposed scheme during an external SLG fault on phase a.

2) Case-2: During External LL fault:

The performance of scheme is tested on external LL fault created between phase a and b at 4.2 s at F_2. Indices $(\mathcal{g}_1^{abc} - \mathcal{g}_2^{abc})$ of phases a, b and c are shown in Fig. 3(a), 3(b), 3(c). Values of $(\mathcal{g}_1^{abc} - \mathcal{g}_2^{abc})$ for phase a, b and c does not exceed ξ. Thus, confirming it as external fault.

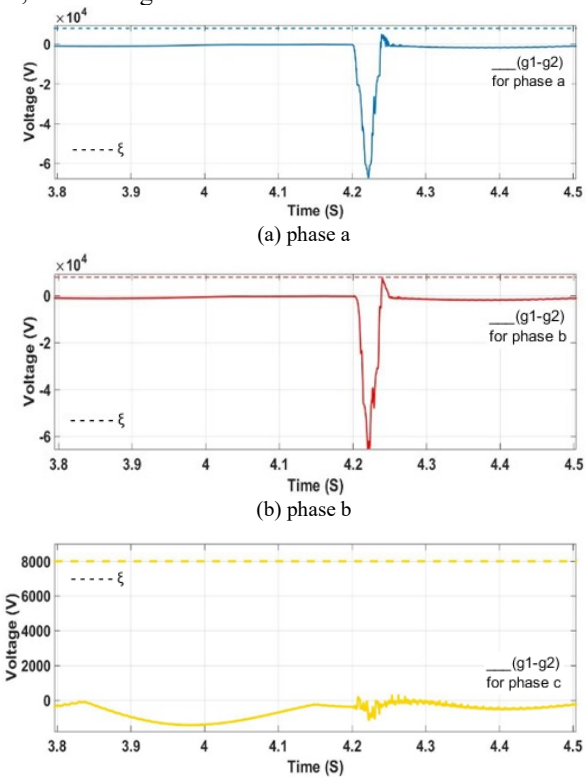

(a) phase a

(b) phase b

(c) phase c

Fig. 3. Performance of proposed scheme during an external LL fault on phase a and b.

3) Case-3: During External LLG fault:

The performance of scheme is tested on external LLG fault created between ground, phase a and phase b at 4.2 s at F_2. Indices $(\mathcal{g}_1^{abc} - \mathcal{g}_2^{abc})$ of phases a, b and c are shown in Fig. 4(a), 4(b), 4(c). Values of $(\mathcal{g}_1^{abc} - \mathcal{g}_2^{abc})$ for phase a, b and c does not exceed ξ. Thus, confirming it as external fault.

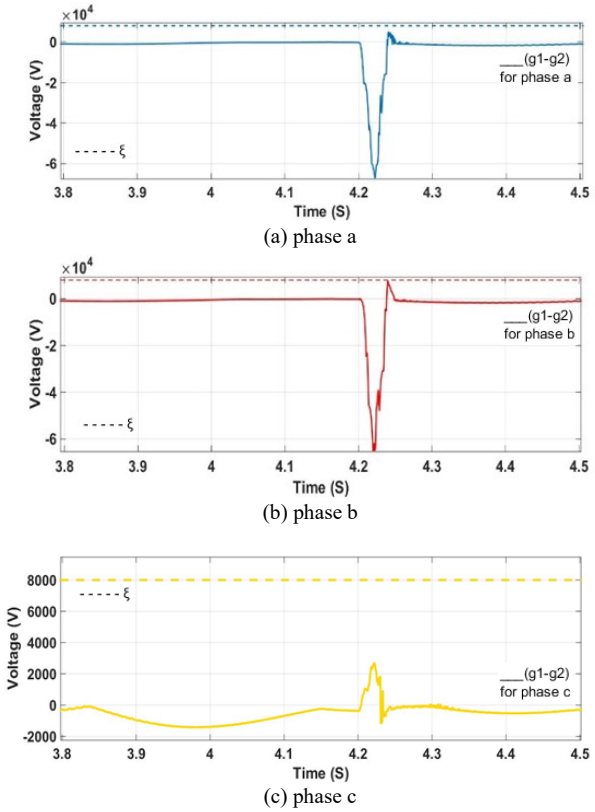

(a) phase a

(b) phase b

(c) phase c

Fig. 4. Performance of proposed scheme during external LLG fault on phases a and b.

4) Case-4: External LLL fault in presence of stable power swing:

The performance of scheme is tested on external LLL fault created at 4.2 s at F_2, 20 km distance from node Q in presence of stable power swing. Fig. 5(a) shows the measured voltage phasors at terminals *M*, *N* and *P* and Fig. 5(b) shows the computed voltage phasors at the *T* point. Indices $(\mathcal{g}_1^{abc} - \mathcal{g}_2^{abc})$ of phases a, b and c are shown in Fig. 5(c), 5(d), 5(e). Values of $(\mathcal{g}_1^{abc} - \mathcal{g}_2^{abc})$ for phase a, b and c does not exceed ξ. Thus, confirming it as external fault.

Simulation results show that the proposed scheme works perfectly in presence of stable power swing.

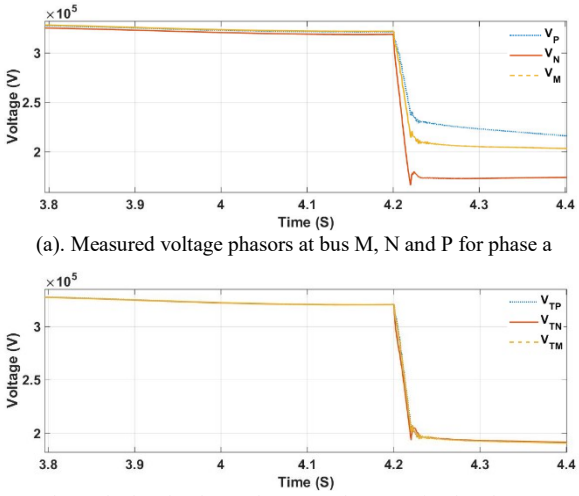

(a). Measured voltage phasors at bus M, N and P for phase a

(b). Calculated voltage phasors at the (T) point for phase a

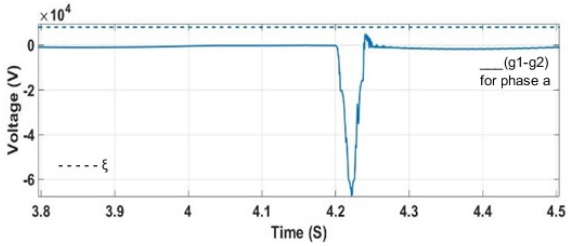

(c) phase a

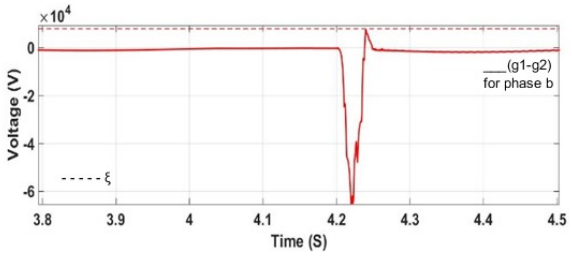

(d) phase b

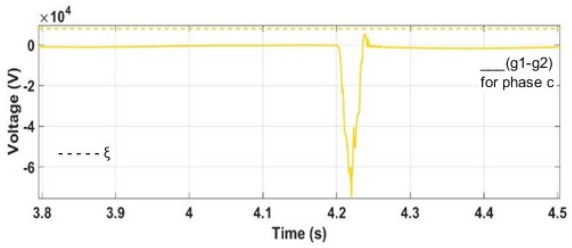

(e) phase c

Fig. 5. Symmetrical external fault performance in presence of stable power swing on phase a, b and c.

5) Performance during faults on an opposite line:

The proposed scheme should perfectly differentiate internal fault and external fault when subjected to any fault condition. Whereas, when fault occurs on opposite parallel line it should indicate the fault as external to the line.

The performance of scheme is tested for faults on an opposite line, LG fault created at 4.2 s at *T'* [on opposite parallel line] of Fig.1. on phase a with fault resistance of 10 Ω. For such a fault, $(\mathcal{g}_1^a - \mathcal{g}_2^a)$ for phase *a* in Fig. 6 is well below ξ hence confirming it as external fault.

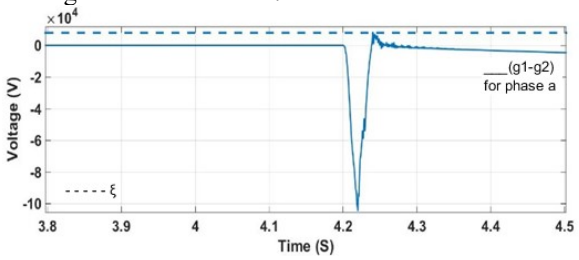

Fig. 6. Performance of proposed scheme during fault on an opposite line.

B. Internal Faults:

The proposed algorithm is tested for various internal faults. The fault location and fault resistance are also varied. We present the results of various internal faults like SLG, LL, LLG, LLL etc. with 10 Ω per phase resistance, created at 20 km distance from node *N* in the direction of (*T*) point at F_1.

1) Case-1: During Internal SLG fault: SLG fault is created on phase a at 4.2 s at F_1. Because it is the internal fault, the value of $(\mathcal{g}_1^a - \mathcal{g}_2^a)$ for phase a exceeds ξ after 12 ms of fault initiation. Fig. 7 shows internal fault at phase a.

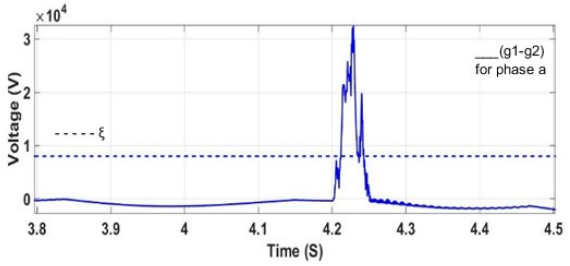

Fig. 7. Performance of proposed scheme during an internal SLG fault on phase a.

2) Case-2: During Internal LL fault:

The performance of scheme is tested on internal LL fault created between phase a and b at 4.2 s at F_1. Indices $(\mathcal{g}_1^{abc} - \mathcal{g}_2^{abc})$ of phases a, b and c are shown in Fig. 8(a), 8(b), 8(c). Values of $(\mathcal{g}_1^{ab} - \mathcal{g}_2^{ab})$ for phase a and b exceeds ξ after 12 ms of fault initiation. Fig. 8(a), 8(b) shows fault at phase a and b. Thus, confirming it as internal fault. Whereas, a value of $(\mathcal{g}_1^c - \mathcal{g}_2^c)$ for phase c does not exceed ξ thus, confirming it as healthy phase.

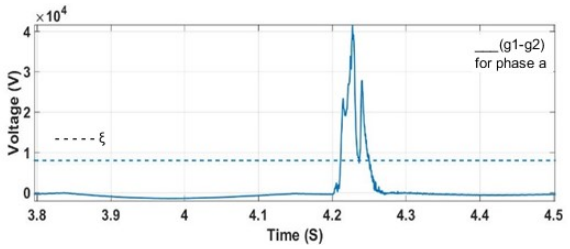

(a) phase a

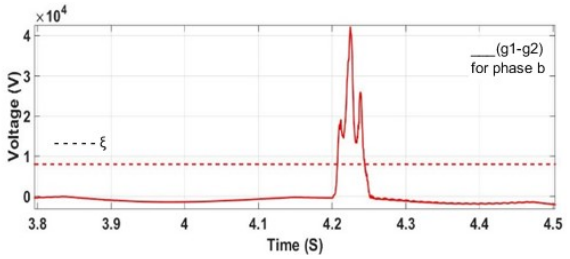

(b) phase b

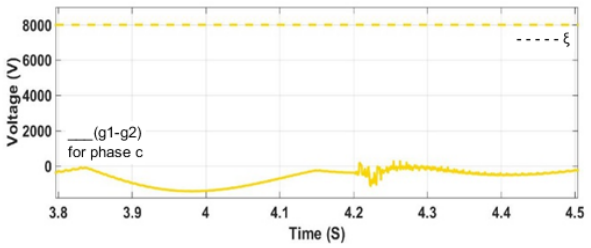

(c) phase c

Fig. 8. Performance of proposed scheme during an internal LL fault on phase a and b.

3) Case-3: During Internal LLG fault:

The performance of scheme is tested on internal for LLG fault created between ground, phase a and phase b at 4.2 s at F_1. Indices $(\mathcal{g}_1^{abc} - \mathcal{g}_2^{abc})$ of phases a, b and c are shown in Fig. 9(a), 9(b), 9(c). Values of $(\mathcal{g}_1^{ab} - \mathcal{g}_2^{ab})$ for phase a and b exceeds ξ after 12 ms of fault initiation. Fig. 9(a), 9(b) shows fault at phase a and b. Thus, confirming it as internal fault. Whereas, a value of $(\mathcal{g}_1^c - \mathcal{g}_2^c)$ for phase c does not exceed ξ thus, confirming it as healthy phase.

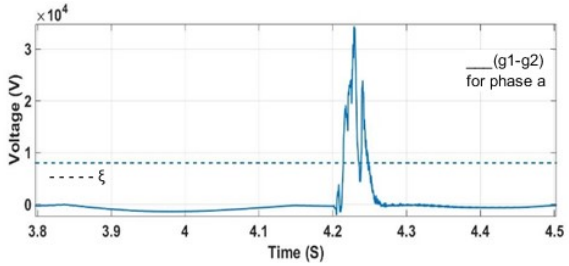

(a) phase a

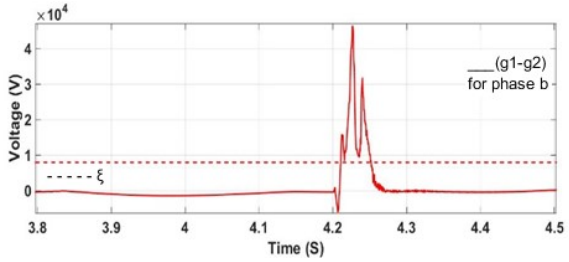

(b) phase b

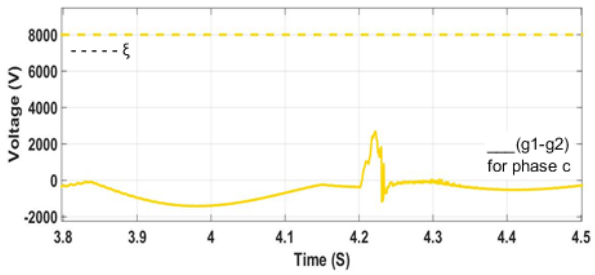

(c) phase c

Fig. 9. Performance of proposed scheme during internal LLG fault on phases a and b.

4) Case-4: Internal LLL fault in presence of stable power swing:

The performance of scheme is tested on internal LLL fault created at 4.2 s at F_1, 20 km distance from node *N* toward the *T* point in presence of stable power swing. Indices ($g_1^{abc} - g_2^{abc}$) of phases a, b and c are shown in Fig. 10(a), 10(b), 10(c). Values of ($g_1^{abc} - g_2^{abc}$) for phase a, b and c exceeds ξ. Thus, confirming it as an internal fault.

Simulation results show that the proposed scheme works perfectly in presence of stable power swing.

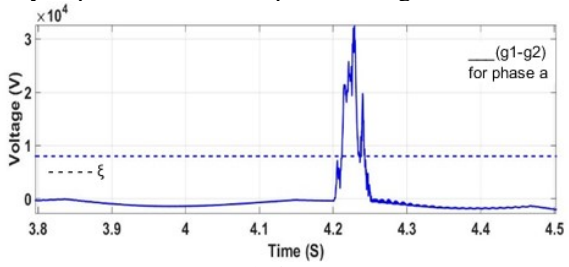

(a) phase a

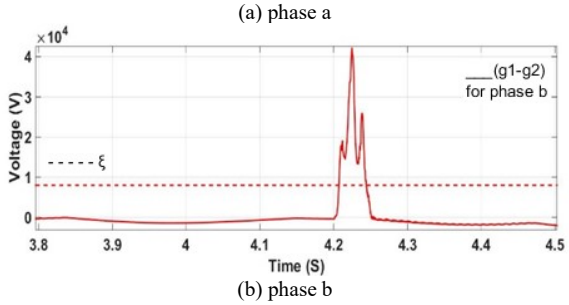

(b) phase b

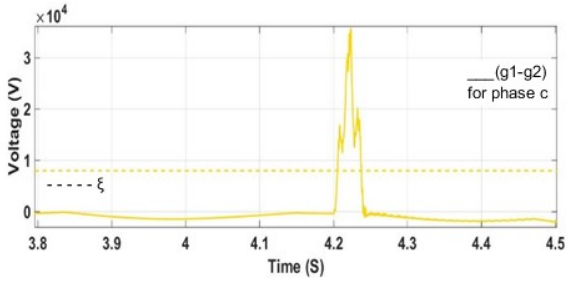

(c) phase c

Fig. 10. Symmetrical internal fault performance in presence of stable power swing on phase a, b and c.

C. *Performance during Faults Near to the T point in presence of stable power swing:*

As the scheme is based on voltage variation at *T* point, the method might be vulnerable when a fault occurs near *T* point. Hence its performance for fault near to *T* point is checked.

1) LLL Fault Near to the T point in presence of stable power swing:

The most severe fault i.e. LLL fault is created near *T* point at 4.2 s. From the Fig. 11, indices ($g_1^{abc} - g_2^{abc}$) for phase a, b and c exceeds ξ after 12 ms of fault initiation. Hence, the scheme works correctly at *T* point in presence of stable power swing.

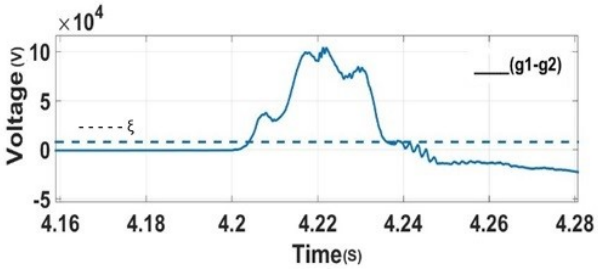

(a). An internal LLL fault performance for all phases

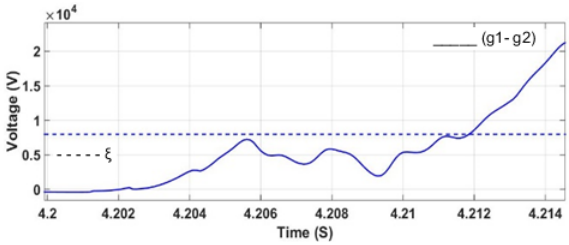

(b). ($g_1^{abc} - g_2^{abc}$) for the inception of the fault

Fig. 11 Performance of proposed scheme during fault near to the *T*-Point.

D. *Large Load Rejection Performance for Proposed Scheme*

The proposed method might be vulnerable when simultaneously subjected to large load rejection and stable power swing. Hence large load rejection is performed at 3 s on a mutually coupled line in presence of stable power swing and system performance is checked and found to be normal as shown in Fig. 12.

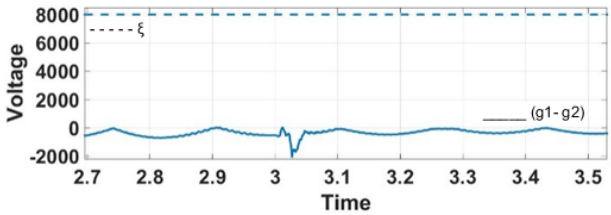

Fig. 12. Performance of proposed scheme during large load rejection.

978-1-5386-6159-8/18/$31.00 ©2018 IEEE

E. *Performance of Proposed Scheme for Fault without Infeed Effect*

The performance of scheme is tested for fault without infeed effect by replacing third source at bus *P* with load. Indices ($\mathcal{g}_1^{abc} - \mathcal{g}_2^{abc}$) of phases a, b and c are shown in Fig. 13. Values of ($\mathcal{g}_1^{abc} - \mathcal{g}_2^{abc}$) for phase a, b and c exceeds ξ. Thus, confirming it as an internal fault.

Simulation results show that the proposed scheme works perfectly for fault without infeed effect.

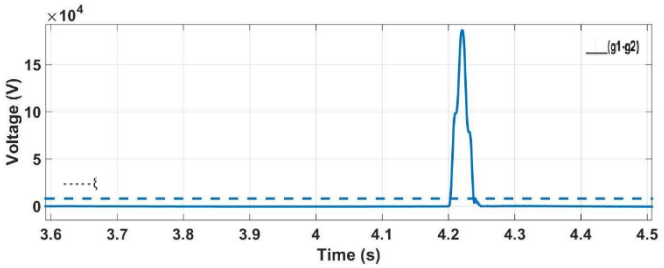

Fig. 13. Performance of proposed scheme during fault without infeed effect.

V. CONCLUSION

A superimposed component of voltage based technique is presented in this paper for protecting three-terminal mutually coupled double-circuit transmission lines in phase domain. The method compares the maximum of superimposed voltage phasor components calculated at the tap point with the maximum of superimposed voltage phasor components measured at the three terminals of the line. The proposed method correctly differentiates internal and external faults. The proposed method correctly differentiates symmetrical fault from stable power swing and is simple to implement.

REFERENCES

[1] IEEE Guide for Protective Relay Applications to Transmission Lines C37.113-2015

[2] S. C. Sun and R. E. Ray, "Development of a PCM using current differential relay systems using fiber optics communications," IEEE Transactions on Power Apparatus and Systems, vol. PAS-102, no. 2, pp. 410–419, Feb. 1983.

[3] "Network Protection and Automation Guide," 1st edition Areva T&D, Paris, France, Mar 11, 2016. [Online]. Available: www.alstom.com

[4] "The complexity of protecting three-terminal transmission lines,"-- NERC 2006. [Online]. Available: www.nerc.com

[5] Paresh Kumar Nayak, Ashok Kumar Pradhan: 'A Three-Terminal Line Protection Scheme Immune to Power Swing', IEEE Transactions on Power Delivery, 2016

[6] Snehal V. Unde, Sanjay S. Dambhare. "PMU based fault location for double circuit transmission lines in a modal domain", 2016 IEEE Power and Energy Society General Meeting (PESGM), 2016, Bosten USA

[7] Pratim Kundu, Ashok Kumar Pradhan. "Wide Area backup protection using weighted apparent impedance", 2015 IEEE Power, Communication and Information Technology Conference (PCITC), 2015, Bhubanesvar India

[8] Al-Emadi, Nasser, Amir Ghorbani, and Hasan Mehrjerdi. "Synchrophasor-based backup distance protection of multi-terminal transmission lines" , IET Generation Transmission & Distribution, 2016.

[9] Snehal V. Unde, Sanjay S. Dambhare. "Differential protection of mutually coupled lines in modal domain using synchronized measurements", 2016 National Power Systems Conference (NPSC), 2016, Bhubanesvar India

[10] Dambhare, Sanjay, S. A. Soman, and M. C. Chandorkar. "Current Differential Protection of Transmission Line Using the Moving Window Averaging Technique", IEEE Transactions on Power Delivery, 2010.

APPENDIX

System parameters are as follows.

Generator G_1: 22 kV, 1 GVA, 50 Hz.

With 6.4 s inertia constant

Generator G_2: 22 kV, 0.4 GVA, 50 Hz.

With 3.5 s inertia constant

Infinite bus-Q: 400 kV, 20 GVA, 50 Hz.

Transformers:

T_1: Y-Y, 3-phase, 22/400 kV, 1.0 GVA, 50 Hz.

T_2: Y-Y, 3-phase, 22/400 kV, 0.4 GVA, 50 Hz.

T_1 and T_2 are grounded on both Y-sides.

Transmission line parameter:

$Z_1 = 0.3286\ \Omega/\text{km}\angle 84.25^0$ $Z_0 = 1.3333\ \Omega/\text{km}\angle 76.6^0$

$C_1 = 11.36$ nF/km, $C_0 = 6.9$ nF/km

$Z_{mutual} = 0.947\ \Omega/\text{km}\angle 79.2^0$